Effect of hydrostatic pressure on phase transitions in $ABF_6.6H_2$ crystals (A identical to Zn,Co,Mg,Mn,Fe:B identical to Ti,Si)

1992 J. Phys.: Condens. Matter 4 91

(http://iopscience.iop.org/0953-8984/4/1/020)

J. Phys.: Condens. Matter 4 (1992) 91–99. Printed in the UK

Effect of hydrostatic pressure on phase transitions in $ABF_6 \cdot 6H_2O$ crystals(A ≡ Zn, Co, Mg, Mn, Fe; B ≡ Ti, Si)

I N Flerov, M V Gorev, K S Aleksandrov and M L Afanasyev
L V Kirensky Institute of Physics, Krasnoyarsk 660036, USSR

Received 12 April 1991, in final form 4 July 1991

Abstract. The effect of hydrostatic pressure on structural phase transitions in some fluorotitanates and fluorosilicates of the $ABF_6 \cdot 6H_2O$ family is studied. It is shown that it is possible to divide the crystals of this family into two groups differing from each other in their values of entropy change and shifts of the phase transition temperature T_0 under pressure. In some compounds the high-pressure phases and triple points were established. The phase diagram for $FeSiF_6 \cdot 6H_2O$ can be considered as a unified diagram describing the possible phase transitions in the crystals studied. The effect of deuteration is investigated in different phases.

1. Introduction

Structural phase transitions (PTs) in fluoride crystals with general formula $ABF_6 \cdot 6H_2O$ (A ≡ Ni, Co, Zn, Mg, Mn, Fe, Cd; B ≡ Si, Ti, Ge, Zr) have been studied up to now by many investigators using different physical methods [1–19]. The rhombohedrally distorted CsCl-type structure of these compounds consists of octahedra of two kinds, namely $[A \cdot 6H_2O]^{2+}$ and $[BF_6]^{2-}$. As a rule, both octahedra have almost regular form [1]. On the basis of structural investigations the family $ABF_6 \cdot 6H_2O$ can be divided into two groups. For some of these compounds ($NiSiF_6 \cdot 6H_2O$, $ZnSiF_6 \cdot 6H_2O$, $CoSiF_6 \cdot 6H_2O$, $ZnTiF_6 \cdot 6H_2O$, $CoTiF_6 \cdot 6H_2O$ and $MnTiF_6 \cdot 6H_2O$) the space group was reliably determined to be $R\bar{3}$ ($Z = 1$) [1, 2, 6]. Fluorosilicates of this group unlike fluorotitanates are characterized by the disorder of F atoms between two positions unconnected by any symmetry elements [1, 2]. The second group consists of crystals $FeSiF_6 \cdot 6H_2O$, $MgSiF_6 \cdot 6H_2O$, $MnSiF_6 \cdot 6H_2O$ and $MgTiF_6 \cdot 6H_2O$. Their space groups have not been determined exactly up to now: $R\bar{3}m$ ($Z = 1$) [16, 17], $P\bar{3}m1$ ($Z = 3$) [18], $P\bar{3}$ ($Z = 3$) [3–5]. All crystals mentioned above except nickel and zinc fluorosilicates undergo ferroelastic PTs which are as a rule of first order [1, 9–11, 14, 15, 19]. The symmetry of low-temperature phases is determined as either monoclinic $P2_1/c$ [1, 17] or triclinic $P\bar{1}$ [19]. The analysis of calorimetric data showed the values of entropy change $\Delta S/R$ at PT are different for the two groups of crystals [20]. A large $\Delta S/R$-value of 0.7 or higher is characteristic for the PT $R\bar{3} \rightarrow P2_1/c$. In the second group the entropy change is rather small: $\Delta S/R < 0.5$. The two groups differ also both in their heat capacity and in their birefringence behaviour [20]. Recently in DSC experiments, high-temperature PTs were found in $MgTiF_6 \cdot 6H_2O$ and $MnSiF_6 \cdot 6H_2O$ [20]. At the

0953-8984/92/010091 + 09 $03.50

same time the existence of intermediate phases between the rhombohedral (or trigonal) and monoclinic phases proposed earlier in $CoSiF_6 \cdot 6H_2O$, $CoTiF_6 \cdot 6H_2O$, $ZnTiF_6 \cdot 6H_2O$ [6] and $MgSiF_6 \cdot 6H_2O$ [9] were not confirmed in course of optic and calorimetric investigations [20]. Deuteration of crystals did not lead to significant changes in PT temperature and $\Delta S/R$ [20].

As seen from this short review, in spite of the large number of results it is impossible now to draw conclusion about the reason for the different types of PT in the $ABF_6 \cdot 6H_2O$ family. In fact fluorosilicates and fluorotitanates with the same atom A can belong either to the same group ($CoSiF_6 \cdot 6H_2O$ and $CoTiF_6 \cdot 6H_2O$) or to different groups ($MnSiF_6 \cdot 6H_2O$ and $MnTiF_6 \cdot 6H_2O$). The replacements of A, B and H atoms also change the unit-cell volume as the interaction between atoms. As is well known, the same parameters can be influenced by the external stress. This type of study, can help to throw light upon the mechanism of PTs.

The present paper is devoted to the effect both of hydrostatic pressure on the PTs and of deuteration on the phase diagrams in the two groups of $ABF_6 \cdot 6H_2O$ crystals. Preliminary results were published earlier [21].

2. Experimental details

The PT temperature shift under hydrostatic pressure was measured by means of differential thermographic analysis (DTA). The highly sensitive Ge–Cu thermocouple was used as a differential device with quartz as the standard sample. The temperature of the sample was measured with a copper–constantan thermocouple. The DTA pressure vessel of piston-and-cylinder type associated with the multiplier was filled either with silicone oil or with a mixture of silicone oil with pentane for measurements at low temperatures.

The experiments were performed from 135 to 355 K and from 0 to 600 MPa. The inaccuracy in the phase boundary coordinates was estimated as ±2 K in the temperature and ±10 MPa in the pressure. The details of experimental procedure have been described earlier [22].

3. Results

The p–T diagrams for crystals in the first group are shown in figure 1. For all the studied compounds the PT temperature T_0 between the rhombohedral ($R\bar{3}$) and monoclinic ($P2_1/c$) phases decreases with pressure increase. The values of T_0 shift under pressure in $ZnTiF_6 \cdot 6H_2O$ ($dT_0/dp = -0.25 \pm 0.04$ K MPa^{-1}) and $MnTiF_6 \cdot 6(H_{0.5}D_{0.5})_2O$ ($dT_0/dp = -0.29 \pm 0.04$ K MPa^{-1}) are close to each other and significantly less than $dT_0/dp = -0.82 \pm 0.17$ K MPa^{-1} for $CoSiF_6 \cdot 6H_2O$. The large difference between the dT_0/dp-values for the same type of PT in fluorotitanates and fluorosilicates may be connected in particular with peculiarities of the crystal structure mentioned above [1, 2]. The sign of dT_0/dp for cobalt fluorosilicate does not confirm the results of experiments at uniaxial pressure [23] where $dT_0/d\sigma_c$ was found to be positive and it was proposed that T_0 did not change for compression along other axes. For $ZnTiF_6 \cdot 6H_2O$ a decrease in T_0 can also be obtained from the Clapeyron–Clausius equation $dT_0/dp = \delta V/\delta S \simeq -0.1$ K MPa^{-1} using both thermal dilatation [24] and calorimetric [20, 21] data. The difference between the calculated and the measured values of dT_0/dp is connected with the difficulties of volume jump determination [24].

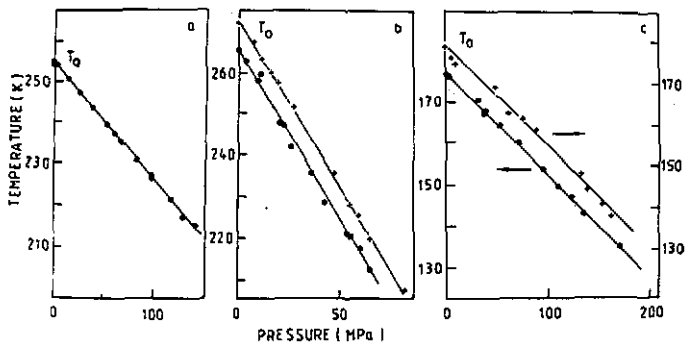

Figure 1. Pressure dependence of PT temperatures for (*a*) $MnTiF_6 \cdot 6(H_{0.5}D_{0.5})_2O$ (●, $x = 0$), (*b*) $CoSiF_6 \cdot 6(H_{1-x}D_x)_2O$ (●, $x = 0$; +, $x = 0.9$) and (*c*) $ZnTiF_6 \cdot 6(H_{1-x}D_x)_2O$ (●, $x = 0$; +, $x = 0.53$).

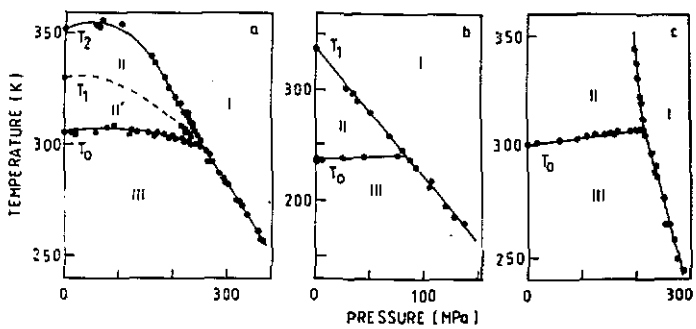

Figure 2. p–T phase diagrams: (*a*) $MgTiF_6 \cdot 6H_2O$; (*b*) $MnSiF_6 \cdot 6H_2O$; (*c*) $MgSiF_6 \cdot 6H_2O$.

The effect of deuteration on T_0 shift under pressure was investigated for $ZnTiF_6 \cdot 6(H_{0.47}D_{0.53})_2O$ and $CoSiF_6 \cdot 6(H_{0.1}D_{0.9})_2O$ crystals (see figures 1(*b*) and 1(*c*)). The changes in dT_0/dp-value did not exceed about 2%.

The phase diagrams for crystals of the second group are individual and rather complicated, as seen in figure 2. Their general feature is the increase in PT temperature T_0 ($R\bar{3}m$, $P\bar{3}m1$, $P\bar{3}$) → ($P2_1/c$, $\bar{1}$) with increase in pressure unlike the situation in the first group of crystals.

For $MgTiF_6 \cdot 6H_2O$ this peculiarity is characteristic of the initial slopes both for dT_0/dp at $p \leqslant 100$ MPa and apparently for another two high-temperature PTs at T_1 and T_2. During the experiments the anomaly in the heat capacity, connected with the PT at $T_1 = 330$ K, was detected only at $p = 0$ and $p \geqslant 200$ MPa. Therefore the boundary between these two phases is shown by a broken curve in figure 2(*a*). It is a pity that we could not detect the point where the line of the II–II′ PT met either the I–II phase boundary or the II′–III boundary. The I–II and II′–III phase boundaries approach each other with increasing pressure and meet at the I–II′–III triple point characterized by the following parameters: $T_{tr} = 302$ K and $p_{tr} = 243$ MPa. As seen in figure 2(*a*), the I–III phase boundary is linear with the coefficient $dT_{I-III}/dp = -0.36 \pm 0.08$ K MPa^{-1}. The values of the shifts in other PT temperatures in magnesium fluorotitanate change in the following intervals: dT_{I-II}/dp from +0.10 to −0.42 K MPa^{-1} and $dT_{II'-III}/dp$ from +0.05 to −0.04 K

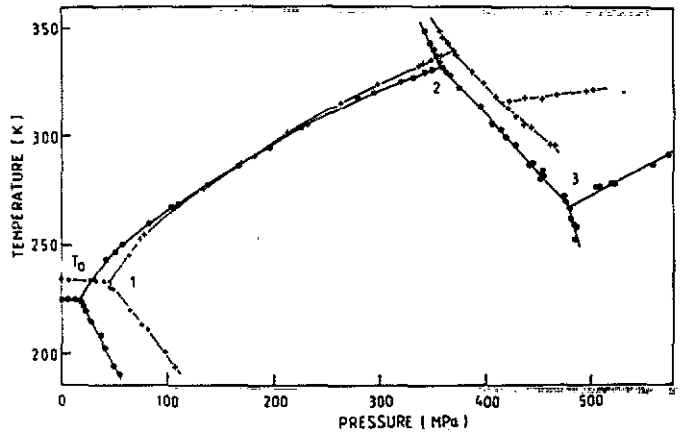

Figure 3. Effect of both pressure and deuteration on $FeSiF_6 \cdot 6(H_{1-x}D_x)_2O$: ●, samples with $x = 0$; +, samples with $x = 0.5$; 1, 2, 3, triple points.

MPa^{-1}. For this crystal, DTA experiments under pressure as well as calorimetric measurements were carried out on two types of sample with high and low temperatures of decomposition [20, 21]. In both cases the phase diagrams coincide at $p > 0$.

The triple point was also found in the phase diagram of $MnSiF_6 \cdot 6H_2O$ undergoing two PTs at $p = 0$ [20] with parameters $T_{tr} = 241$ K and $p_{tr} = 80$ MPa (see figure 2(*b*)). All phase boundaries are linear with the following slopes: $dT_{I-II}/dp = -1.12 \pm 0.21$ K MPa^{-1}; $dT_{II-III}/dp = +0.06 \pm 0.05$ K MPa^{-1}; $dT_{I-III}/dp = -1.12 \pm 0.20$ K MPa^{-1}.

As known from optic and calorimetric investigations of $MgSiF_6 \cdot 6H_2O$, this crystal has one PT at ambient pressure up to the decomposition temperature [20]. It is seen from figure 2(*c*) that the high-pressure phase exists in this crystal. The triple point was taken to be at $T_{tr} = 308$ K and $p_{tr} = 217$ MPa. The slopes of the phase boundaries are characterized by the following values: $dT_{I-II}/dp = -1.92 \pm 0.58$ K MPa^{-1}; $dT_{I-III}/dp = -0.90 \pm 0.17$ K MPa^{-1}; $dT_{II-III}/dp = +0.03 \pm 0.02$ K MPa^{-1}.

$FeSiF_6 \cdot 6H_2O$ has the most complicated phase diagram of the crystals in the second group (figure 3). Three triple points were found during measurements from 190 to 350 K and from 0 to 600 MPa. Their coordinates are as follows: $T^1_{tr} = 226$ K, $p^1_{tr} = 17$ MPa; $T^2_{tr} = 333$ K, $p^2_{tr} = 358$ MPa; $T^3_{tr} = 268$ K, $p^3_{tr} = 480$ MPa. The effect of deuteration on the phase diagram was studied using the $FeSiF_6 \cdot 6(H_{0.5}D_{0.5})_2O$ sample (figure 3). It is necessary to point out that T_0 remains almost constant for both normal and deuterated crystals up to 17 MPa and 44 MPa, respectively. Recently such a situation was observed during x-ray and DTA experiments under pressure up to 20 MPa [25]. The triple point was found at $p_{tr} = 7.5$ MPa. Thus from our point of view it is difficult to attribute $FeSiF_6 \cdot 6H_2O$ to either group of this family because of the intermediate value of the total entropy change $\Delta S_0 = 0.51R$ for the PT at ambient pressure [20, 21] and the absence of a T_0 shift under pressure.

4. Discussion

The appearance and alternation of different phases in crystals at the change in temperature and pressure are conditioned by ion interactions which depend on the distances

Table 1. The unit-cell volumes of fluorosilicates and fluorotitanates $ABF_6 \cdot 6H_2O$ in the trigonal phase. $V = (3\sqrt{3}/2)a^2c$ ($\times 10^{-30}$ m^3), where a and c are unit-cell parameters in the hexagonal setting, $Z = 3$ [1, 2, 6, 16–18].

	Ni	Zn	Co	Mg	Mn	Fe
$ASiF_6 \cdot 6H_2O$	722.7	735.3	739.0	767.7	769	774.7
$ATiF_6 \cdot 6H_2O$	781.0	790.0	795.3		820.0	821.7

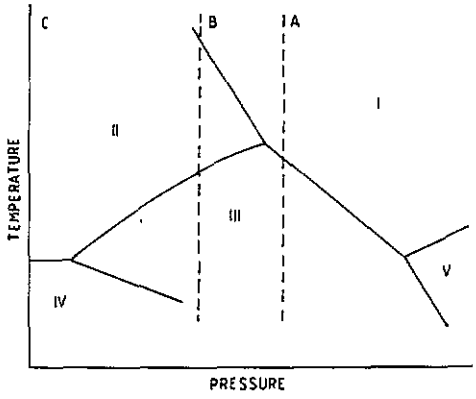

Figure 4. The generalized p–T phase diagram of the $ABF_6 \cdot 6H_2O$ family. A is the part of the diagram observed with crystals in the first group; B is the part characteristic of the second group; C is the full hypothetical phase diagram.

between them. These distances can be characterized for example by the value of the unit-cell volume. Under pressure the volume decreases and the crystal can behave similar to another one from the same family with a smaller initial volume. Thus a hypothetical crystal may exist which has the p–T diagram for the whole family of crystals. There are several examples of this [26, 27].

The symmetries of the high-temperature and high-pressure phases found in [20] and in the present investigations are not known but, in accordance with the results of the thermodynamic study, one can assume that the phase diagram of $FeSiF_6 \cdot 6H_2O$ includes all PTs known up to now in the $ABF_6 \cdot 6H_2O$ family. The unit-cell volumes V of crystals in the trigonal phase estimated from x-ray data [1, 2, 6, 16–18] are presented in table 1. The comparison of the V-values and individual phase diagrams of different crystals allows one to divide the generalized phase diagram into the characteristic domains (figure 4). Region A is characterized by small values of V, a negative inclination of I–III phase boundary and the presence of triple point I–III–V. The behaviour of T_0 under pressure for the crystals $CoSiF_6 \cdot 6H_2O$, $MnTiF_6 \cdot 6H_2O$ and $ZnTiF_6 \cdot 6H_2O$ corresponds to the PT line I–III in the sign of dT_0/dp and the small influence of deuteration (table 2). One can consider that the triple point can be found at higher pressures.

Region B includes domain A and the triple point I–II–III (figure 4). The positions of phase boundaries in the vicinity of this point correspond to phase diagrams of $MgSiF_6 \cdot 6H_2O$, $MnSiF_6 \cdot 6H_2O$ and apparently $MgTiF_6 \cdot 6H_2O$. The unit-cell volumes of these are larger than the V-values of crystals from region A. The line I–III of crystals

Table 2. The entropy jumps $\delta S/R$ and shifts in PT temperatures under pressure dT_i/dp for $ABF_6 \cdot 6H_2O$ crystals in accordance with the unified phase diagram shown in figure 4. The values $\delta S/R$ are determined for the vicinities of the triple points. The intervals of dT_i/dp changes are given for non-linear boundaries ($d = dT_i/dp$ K MPa^{-1}; $\delta = \delta S/R$.

	I–II		II–III		III–IV		I–III		II–IV		I–V		V–III	
	d	δ	d	δ	d	δ	d	δ	d	δ	d	δ	d	δ
$FeSiF_6 \cdot 6(H_{1-x}D_x)_2O$														
$x = 0$	-1.0 ± 0.5	0.90	0.70 to 0.18	0.27	-0.94 ± 0.32	0.15	-0.51 ± 0.07	1.2	0 ± 0.2	0.38	0.27 ± 0.07	0.48	-1.75 ± 0.50	0.26
$x = 0.5$	-0.8 ± 0.4		0.65 ± 0.22		-0.63 ± 0.18		-0.50 ± 0.18		0 ± 0.1		0.07 ± 0.05		-0.42 ± 0.12	
$MnSiF_6 \cdot 6H_2O$	-1.12 ± 0.21	0.46	0.06 ± 0.05	0.20[a]			-1.12 ± 0.20	0.6						
$MgSiF_6 \cdot 6H_2O$	-1.92 ± 0.58	0.40	0.03 ± 0.02	0.40[a]			-0.90 ± 0.17	1.1						
$MgTiF_6 \cdot 6H_2O$	0.1 to −0.4	0.84	0.05 to −0.04	0.28[a]			-0.36 ± 0.08	1.68						
$MnTiF_6 \cdot 6(H_{0.5}D_{0.5})_2O$							-0.29 ± 0.04	0.83						
$CoSiF_6 \cdot 6(H_{1-x}D_x)_2O$														
$x = 0$							-0.82 ± 0.17	0.64[a]						
$x = 0.9$							-0.82 ± 0.16	0.75						
$ZnTiF_6 \cdot 6(H_{1-x}D_x)_2O$														
$x = 0$							-0.25 ± 0.04	0.95[a]						
$x = 0.53$							-0.25 ± 0.04	0.94[a]						

[a] These $\delta S/R$ values determined using an adiabatic calorimeter [14, 15, 20, 21].

in the second group is characterized by a negative slope and different values of dT_{I-III}/dp for fluorotitanates and fluorosilicates similar to the dT_0/dp-value for compounds in the first group (table 2). It is reasonable to suppose that the absence of a PT for the fluorosilicates of Zn and Ni is determined by the very small volumes of the unit cells and the large negative slope of the PT I–III line.

Region C in figure 4 presents the diagram of $FeSiF_6 \cdot 6H_2O$ characterized by the largest volume of the crystals studied (table 1). Probably phase IV may exist in crystals with smaller V. Recently an additional PT somewhere between 30 and 10 K was detected through the EPR measurements [28].

The heat capacity measurements made with an adiabatic calorimeter on crystals studied in the present paper were carried out in [14, 15, 20, 21]. It was found that at ambient pressure the strong first-order PTs in crystals in the first group were characterized by equivalency of the values of the total entropy change ΔS and of the entropy jump δS at the PT temperature. For crystals in the second group, δS is about 0.7 ΔS. PTs into high-temperature and high-pressure phases are also of first order. Using the DTA method to measure the PT temperature shift under pressure we could at the same time obtain information only about the entropy jumps δS through transitions. The areas of peaks on the DTA curves remain constant with pressure increase. This means that the values of the entropy jumps δS for the PTs investigated did not depend on pressure. It allowed us to determine the values δS for transformations into high-pressure phases by comparison of corresponding areas of the DTA curve peaks with the same areas of the PTs investigated using an adiabatic calorimeter [14, 15, 20, 21]. The inaccuracy in the entropy jumps δS was estimated to be about 30%. As seen from table 2 each line in the unified phase diagram in figure 4 is characterized by a corresponding value of δS and, in the vicinities of the triple points, $\delta S_{I-III} = \delta S_{I-II} + \delta S_{II-III}$, $\delta S_{I-III} = \delta S_{I-V} + \delta S_{V-III}$ and $\delta S_{II-IV} = \delta S_{II-III} + \delta S_{III-IV}$ for the first-order PTs are obtained just by taking into consideration the inaccuracy in δS mentioned above.

If the assumption about the unified phase diagram shown in figure 4 is real, one can assume the following symmetries of phases. The space group $R\bar{3}$ in phase I was reliably determined for many crystals [1, 2, 29]. The symmetry of phase II is the most uncertain and one can say only that the crystals in it belong to point group $\bar{3}$ [3–5, 16–18]. Phase III is monoclinic with the space group $P2_1/c$ [17]. According to recent optical investigations of $FeSiF_6 \cdot 6H_2O$ [19], phase IV in figure 4 may be triclinic $P\bar{1}$. The symmetry of phase V is uncertain because it was not yet observed at ambient pressure in any crystals in the family.

The space group $P2_1/c$ is not a subgroup of $R\bar{3}$ [30]; therefore both of them are distorted variants of some high-symmetry parent phase (G_0). The cubic structure with $G_0 = Pm3m$ ($Z = 1$) can be chosen as the parent phase of rhombohedrally distorted CsCl-type structure (phase I in figure 4). The hydrogen, oxygen and fluorine atoms can be disordered in G_0. PTs into both $R\bar{3}m$ ($Z = 1$) and $R\bar{3}$ ($Z = 1$) subgroups are possible depending on the type of distortion. The first case is connected with compression of the unit cell along one of threefold axes. In the course of the $Pm3m \rightarrow R\bar{3}$ PT this deformation is accompanied by tilts of the octahedra. Judging by the slope of line I–II in figure 4 it is difficult to imagine that phase II belongs to space group $R\bar{3}m$ where unlike $R\bar{3}$ the disorder of fluorine and oxygen atoms exists. The reasons for the appearance of disorder on decrease in temperature are unclear. Thus the $R\bar{3}m$ phase can only be intermediate between the $R\bar{3}$ and $Pm3m$ phases. The hydrogen bonds are partially ordered in this phase. The ordering of hydrogen bonds can be increased during PTs owing to the mutual tilts of $[A \cdot 6H_2O]^{2+}$ and $[BF_6]^{2-}$ octahedra. The distorted phases are subgroups of $R\bar{3}m$, and PTs can be described within the framework of the thermodynamic theory [31].

Between $R\bar{3}$ and $P2_1/c$ the group-to-subgroup relation does not exist, so that the PT from the rhombohedral into the monoclinic phase should be of strong first-order nature, which is confirmed by calorimetric experiments on $CoZrF_6 \cdot 6H_2O$ and $ZiTiF_6 \cdot 6H_2O$ [15, 20]. The analysis of the II–III and II–IV PTS is impossible because of unreliable determination of the symmetry of phase II.

The PTS considered above are connected with the octahedra tilts. The minor role of hydrogen bonds in these transformations is supported by the results of investigations on deuterated crystals. The effect of deuteration on the entropy change, T_0 and dT_0/dp is small (table 2, figures 1(*b*), 1(*c*) and 4). At the same time there is a large difference between the parameters of the triple point I–III–V and the dT_{III-IV}/dp, dT_{I-V}/dp- and dT_{V-III}/dp-values for normal and deuterated $FeSiF_6 \cdot 6H_2O$. This means that the III–IV, I–V and V–III PTS are possibly accompanied by changes in the hydrogen bond system.

5. Conclusions

Experimental studies on the $ABF_6 \cdot 6H_2O$ family performed in the present paper and in [21] have shown the existence of crystals with different types of structural PTS. In some compounds, high-temperature and high-pressure phases and triple points were found. Either unique or successive PTS were realized on temperature and pressure changes. The phase diagram of $FeSiF_6 \cdot 6H_2O$ includes apparently all possible PTS in the family and can be considered as a generalized diagram for the whole family.

Acknowledgments

The authors wish to thank Mrs V S Abakumova for help in growing the crystals, Mrs N B Levchuk for technical assistance and Dr E P Zeer for discussion of the results.

References

[1] Chattopadhyay T, Devreux E, Peters K, Peters E-M, Gmelin E and Ghosh B 1988 *J. Phys. C: Solid State Phys.* **21** 1321
[2] Ray S, Zalkin A and Templeton D H 1973 *Acta Crystallogr.* B **29** 2741
[3] Jehanno G and Varret F 1975 *Acta Crystallogr.* A **31** 857
[4] Chevrier G and Jehanno G 1979 *Acta Crystallogr.* A **35** 912
[5] Chevrier G and Jehanno G 1981 *Acta Crystallogr.* A **37** 578
[6] Bose M, Roy K and Ghoshray R 1987 *Phys. Rev.* B **35** 6619
[7] Afanasyev M L, Lybzikov G P, Menshikov V V and Zeer E P 1979 *Chem. Phys. Lett.* **60** 279
[8] Rubins R S and Kwee K K 1977 *J. Chem. Phys.* **66** 3948
[9] Ziatdinov A M, Kuryavy V G and Davidovich R L 1985 *Fiz. Tverd. Tela* **27** 2152
[10] Ziatdinov A M, Kuryavy V G and Davidovich R L 1986 *Fiz. Tverd. Tela* **28** 3549
[11] Ziatdinov A M, Kuryavy V G and Davidovich R L 1987 *Fiz. Tverd. Tela* **29** 215
[12] Choudhury P, Ghosh B, Lamba O P and Bist H B 1983 *J. Phys. C: Solid State Phys.* **16** 1609
[13] Choudhury P, Ghosh B, Patel M B and Bist H B 1984 *J. Phys. C: Solid State Phys.* **17** 5827
[14] Weir R D, Halstead K E and Staveley L A K 1980 *Discuss. Faraday Soc.* **69** 202
[15] Weir R D, Halstead K E and Staveley L A K 1985 *J. Chem. Soc. Faraday Trans.* II **81** 189
[16] Hamilton W C 1962 *Acta Crystallogr.* **15** 353
[17] Syoyama S and Osaki K 1972 *Acta Crystallogr.* B **28** 2626
[18] Kodera E, Torii A, Osaki K and Watanabe T 1972 *J. Phys. Soc. Japan* **32** 863

[19] Eremenko V V, Peschansky A V and Fomin V I 1989 *Kristallografiya* **34** 658
[20] Flerov I N, Gorev M V, Melnikova S V, Afanasyev M L and Aleksandrov K S 1991 *Fiz. Tverd. Tela* **33** 1921
[21] Flerov I N, Gorev M V, Melnikova S V, Afanasyev M L and Aleksandrov K S 1990 *Preprint* 654F, Kirensky Institute of Physics, Krasnoyarsk
[22] Gorev M V 1983 *Fiz. Tverd. Tela* **25** 566
[23] Datta Roy S K, Pal A, Ghosh B, Chattorje M and Das A M 1977 *J. Phys. C: Solid State Phys.* **10** L403
[24] Choudhury P, Mandal P, Das A M and Ghosh B 1986 *J. Phys. C: Solid State Phys.* **19** 3961
[25] Asadov S K, Zavadsky E A, Kamenev V I and Todris B M 1990 *Fiz. Tverd. Tela* **32** 2420
[26] Andersson P and Ross R G 1987 *J. Phys. C: Solid State Phys.* **20** 4737
[27] Braud M N, Couzi M, Chanh N B, Courseille C, Gallois B, Hauw C and Meresse A 1991 *J. Phys.: Condens. Matter* **2** 8209
[28] Rubbins R S, Drumheller J E and Hutton S L 1989 *J. Chem. Phys.* **91** 3614
[29] Chevrier G and Saint-James R 1990 *Acta Crystallogr.* C **46** 186
[30] Toledano P and Toledano J-C 1977 *Phys. Rev.* B **16** 387
[31] Lybzikov G P, Flerov I N, Iskornev I M, Afanasyev M L, Zeer E P and Aleksandrov K S 1982 *Nuclear Magnetic Relaxation and Dynamics of Spin Systems* ed K S Aleksandrov (Krasnoyarsk: Kirensky Institute of Physics) pp 15–32